Delayed Data Acquisition for Optimal PET Activation Studies with Oxygen-15-Water in Cerebral Arteriovenous Malformation

Hidehiko Okazawa, Yoshiharu Yonekura, Norihiro Sadato, Hugh Lyshkow, Sadahiko Nishizawa, Reinin Asato, Yasuhiro Magata, Koichi Ishizu, Nagara Tamaki, Junji Konishi and Haruhiko Kikuchi

Departments of Nuclear Medicine, Brain Pathophysiology and Neurosurgery, Kyoto University, Kyoto, Japan

In the clinical application of activation PET studies with ^{15}O-water, optimal PET images are required when the high activity of a nearby lesion might affect the activated area. **Methods:** To determine the optimal time for data acquisition of PET images, we performed serial dynamic PET measurements in five patients with cerebral arteriovenous malformation (AVM). All AVMs were closest to the motor cortices, and the activation task was opponent finger movement contralateral to the AVM. Activation PET and MR images were coregisterated for localization of activated foci. **Results:** Time-activity curves of the nidus and normal cortex from the dynamic PET data demonstrated a discrepancy in peak time and significant radioactivity increase in the nidus during the early phase. Elimination of the initial PET data provided better contrast in activated foci without affecting the calculated cerebral blood flow of other areas. **Conclusion:** Delayed data acquisition can avoid interference of the AVM nidus with the activated area.

Key Words: arteriovenous malformation; cerebral blood flow; positron emission tomography; activation studies

J Nucl Med 1995; 36:2149–2153

One of the useful clinical approaches of activation PET studies is to visualize the location and relationship between brain lesions and activated foci. Coregistration of PET and MR images has proved to be a useful method for determining the best treatment of cerebral arteriovenous malformation (AVM) in functionally important cortices (*1,2*). Since the proximity of cerebral AVM to critical brain regions is one of the major risk factors that might affect the surgical results, we should consider their anatomical location precisely. The increased activity of the nidus, however, interferes with signals in the activated area, especially in case of close location.

Although the optimal scan time of the autoradiographic method using ^{15}O-water has already been reported in several articles (*3–6*), abnormally high activity in the brain due to large vascular lesions has not been addressed. To obtain optimal PET images in patients with cerebral AVM, we analyzed the effects of delayed data acquisition on the nidus and activated area in five patients with AVMs in close location to the motor cortices.

Received Aug. 19, 1994; revision accepted Mar. 6, 1995.

For correspondence or reprints contact: Hidehiko Okazawa, MD, Department of Nuclear Medicine, Kyoto University Faculty of Medicine, 54 Shogoin Kawahara-cho, Sakyo-ku, Kyoto 606-01, Japan.

MATERIALS AND METHODS

Patients

We studied five patients with cerebral AVM (3 men, 2 women, aged 21–54 yr). All patients were right-handed and had been referred because of neurological symptoms (Table 1). The nidus in each patient was located adjacent to the motor cortices. One patient suffered from moderate left hemiparesis due to the rupture of the AVM (Patient 2), but motor weakness improved when the activation study was performed. Informed consent was obtained from each patient before the PET study.

PET

We used a PET system that permits simultaneous acquisition of 15 transverse slices with a center-to-center distance of 7 mm and axial resolution of 6.5 mm FWHM at the center (*7,8*). The in-plane spatial resolution with stationary mode acquisition was 6.7 mm FWHM, which was blurred to about 9 mm on the reconstructed PET images. The field of view and pixel size were 256 and 2 mm, respectively.

Prior to all emission measurements, tomographic transmission data were obtained using a $^{68}Ge/^{68}Ga$ standard plate source for attenuation correction. The tissue activity concentration in the PET images was cross-calibrated against the scintillation counter using a cylindrical phantom filled with ^{18}F solution. Before scanning, the head was immobilized using a customized headholder by a fast-hardening foam mold for each patient (*9*). The head was then positioned using laser beams to obtain transaxial slices parallel to the orbitomeatal line.

To measure regional cerebral blood flow (rCBF), approximately 1110 MBq (30 mCi) ^{15}O-water in 6 ml saline were injected into the cubital vein over 15 sec with an automatic injector, and dynamic data acquisition began at the onset of injection for 120 sec in 15-sec frames (*10*).

Functional images of rCBF were calculated using the autoradiographic method with the measured arterial input function (*11,12*), except for Patient 1, in whom the standard arterial input

TABLE 1
Patient Characteristics

Patient no.	Age (yr)	Sex	Symptom	Lesion site
1	23	F	Loss of consciousness	L frontal AVM
2	21	F	Left hemiparesis	R sylvian AVM
3	31	M	Numbness, diplopia	R parietal AVM
4	54	M	Episode of LOC attack	R parietal AVM
5	31	M	Convulsion with LOC	R frontal AVM

LOC = loss of consciousness; AVM = arteriovenous malformation; R = right; L = left

function was used (*10*). In the other four patients, a small cannula was placed in the brachial artery opposite side to the finger task. One milliliter of blood was sampled every 4–5 sec for the first minute after intravenous injection of ^{15}O-water, and then every 10–15 sec for the rest of the imaging session. These blood samples then were immediately processed to measure whole blood radioactivity by a scintillation counter, and the data were used to calculate the absolute rCBF value autoradiographically on a pixel-by-pixel basis (*12*).

Patients were asked to perform simple opponent finger movement contralateral to the AVM at the frequency of twice a second (2 Hz) for the motor activation study (*13*). The task was started 30 sec before administration of ^{15}O-water. Control scans were obtained in the resting condition without any task. Two scans were obtained for each condition. The scan-to-scan interval was 10 to 12 min.

Coregistration of PET and MRI

Before the PET study, MRI was performed in each patient for coregistration of the PET and MR images. MR images were obtained with a head coil covering the whole brain for T1-weighted axial or coronal slices. Each slice thickness was 3 mm without a slice gap. All images were interpolated and reconstructed to a voxel size of 2 × 2 × 2 mm.

After both MRI and PET datasets were rotated axially and coronally to fit the midsagittal plane, PET data were coregistrated to the MRI data by tracing the inner structure and brain contour of the midsagittal and parasagittal section (±10 mm) of the reconstructed MR images individually (*13*). The original 15 slices of the PET dataset were also interpolated to an isotropic volume through linear interpolation to give the same voxel size of the MR images (2 × 2 × 2 mm).

Data Analysis

Four PET images of each subject were first globally normalized to 50 ml/min/100 g whole brain mean blood flow to correct fluctuations of global CBF among successive scans (*14,15*). To avoid the effects of high activity in the nidus during global CBF estimation, the nidus was excluded in the mean CBF calculations. Two images in each condition (resting or finger movement) were averaged, after which the rest images were subtracted from the task images to evaluate activated foci. The subtracted images were superimposed on the individual MR images in the matched location, as determined above, and visually inspected at all available slice levels in the axial and coronal planes.

To evaluate the effect of activity in the nidus to the activated area with increased rCBF, 15-sec dynamic PET data were used to calculate rCBF with various data acquisition times. For each condition, five rCBF images were obtained from the data acquired 0–120 sec, 15–120 sec, 30–120 sec, 45–120 sec and 60–120 sec after starting administration of ^{15}O-water. Regions of interest (ROIs) were set on the site of the nidus and activated area of the motor cortex with the MRI reference. ROIs were also placed on the ipsilateral gray matter close to the activated motor cortex and the contralateral gray matter not affected by the AVM for comparison with activity in the nidus and activated area. Time-activity curves of the nidus and contralateral gray matter were obtained from the dynamic PET data in the control scans of five subjects (10 scans). The activity ratio in the nidus to the contralateral gray matter was also calculated in every frame.

Changes in rCBF values in the nidus, activated foci and ipsilateral adjacent cortex due to the elimination of the initial PET data were calculated using the same ROIs. The ratio of rCBF values in the activated area to that in the adjacent cortex (A/C ratio) was calculated in each control and activation scan for each scan time. The percent increase of the A/C ratio was acquired by dividing the A/C ratio in the control scan by that in the activation scan. The increase in rCBF (ΔCBF) in the activated area and the signal-to-noise (S/N) ratio were also calculated in all rCBF images with different acquisition periods. The S/N ratio was the ratio of increased rCBF value in the activated area to the noise of the peripheral area in the subtracted image. The A/C ratio, percent increase of the A/C ratio, rCBF increases, and the S/N ratio were averaged for every acquisition period. The complete acquisition dataset (120 sec) and each partial acquisition period (15–120 sec to 60–120 sec) were compared and differences were evaluated using analysis of variance (ANOVA). A probability value of less than 0.05 was considered significant.

RESULTS

Activation Study and Coregistration of PET and MRI

Following the motor task, increases in rCBF greater than 20% were observed in the activated foci of all patients. Figure 1 demonstrates the coregistration of the subtracted PET image and MR image of Patient 2. The subtracted PET image superimposed on the MR image clearly showed the activated primary motor area and its adjacent relationship to the AVM. Embolization and direct surgery were performed, and the nidus was completely removed. Although there were no surgical complications, moderate motor weakness of the left upper extremities developed postoperatively. The weakness improved completely within 1 mo.

PET Data Analysis

The time-activity curves of Patient 2 (Fig. 2) show extremely high activity in the AVM nidus in the second and third frames compared to the activity in the contralateral gray matter. The activity peak was seen in the second or third frame in all patients. The average changes of the activity ratio in the nidus to the contralateral gray matter are shown in Figure 3. The activity ratio was significantly higher in the first and second frames than in the other six frames.

Figure 4 shows the effect of elimination of the initial PET data on the rCBF values in the nidus, activated motor cortex and ipsilateral gray matter in the control scan of Patient 2. The rCBF value of the nidus significantly de-

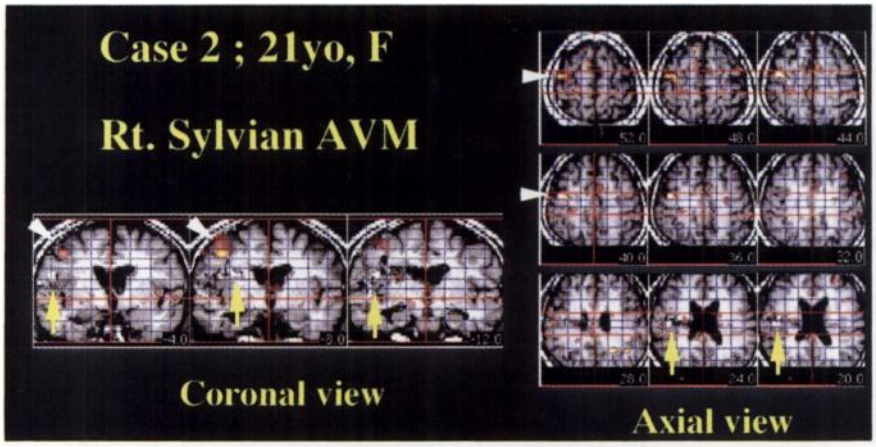

FIGURE 1. Subtracted PET images of Patient 2 superimposed on the MR images in the axial and coronal sections. Coregistration of PET and MRI clearly visualized the activated primary motor area (arrow heads) and its adjacent relationship to the AVM. High signal intensities in the nidus are posthemorrhagic change (arrows). The number at each slice level is the distance (millimeters) from the anterior commissure (AC) -posterior commissure (PC) plane in the axial view and the distance from the AC in the coronal view.

creased when the initial data of 30 sec or more were eliminated. On the other hand, the rCBF value of the ipsilateral gray matter was almost stable, despite shortening the acquisition time. The activated cortical area adjacent to the AVM was severely affected in rCBF by high AVM activity and showed rCBF decreased upon elimination of the initial PET data. This tendency was observed in all patients. Table 2 shows the average changes in the A/C ratio in the task and control scans. Data acquisition of 0–120 sec or 15–120 sec was significantly different with shorter scan times of 45–120 sec or 60–120 sec in both conditions. Elimination of the initial data showed a greater percent increase in the A/C ratio on the activation images.

Figure 5 demonstrates the change in rCBF images with the elimination of the initial PET data. The activity in the nidus decreased gradually when the initial data were eliminated without affecting rCBF in other areas.

Table 3 shows the changes in ΔCBF and the S/N ratio in the activated area after elimination of the initial data. Each measure severely decreased when three or more frames of the initial dynamic data were eliminated. For the S/N ratio change, a significant decrease was observed with elimination of the initial 45- or 60-sec data when compared with the 0–120-sec acquisition.

DISCUSSION

PET activation studies with coregistration to individual MR images are reportedly one of the most useful methods for determining the optimum treatment for cerebral AVM (*1,2*), especially when there is close proximity to the func-

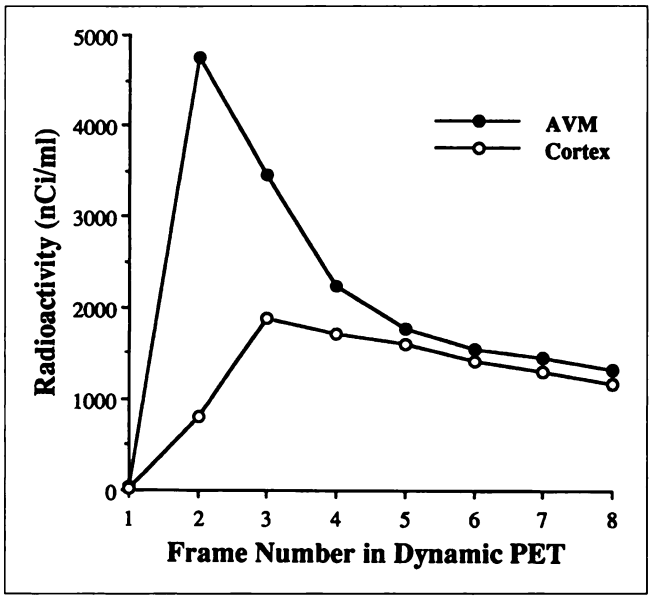

FIGURE 2. Time-activity curves of Patient 2 demonstrate extremely high activity in the AVM nidus in the second and third frames compared to activity in the contralateral gray matter. The activity peak seen in the second frame was earlier than the peak for contralateral gray matter.

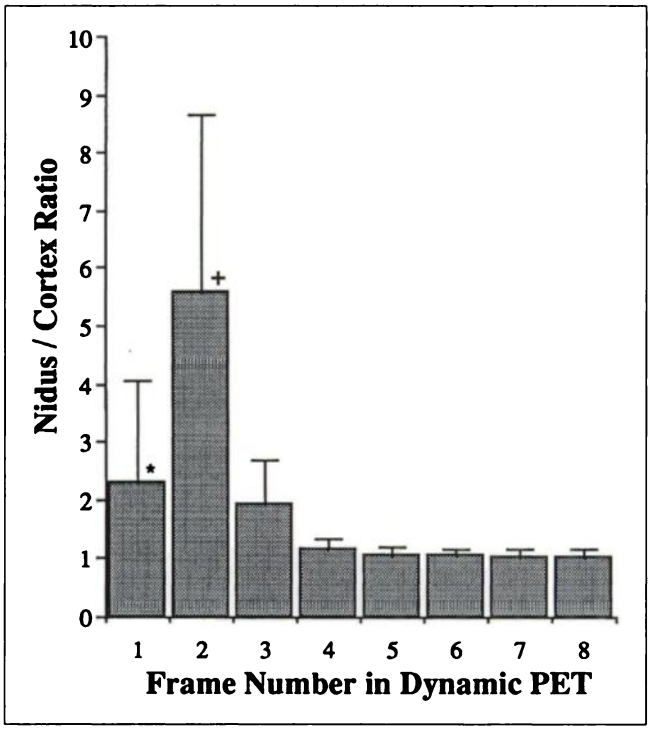

FIGURE 3. Average activity ratio changes in the nidus to the contralateral gray matter. Values are the mean of 10 control studies. The activity ratio was significantly higher in the first and second frames than in the other six frames. *$p \leq 0.05$; †$p \leq 0.0001$.

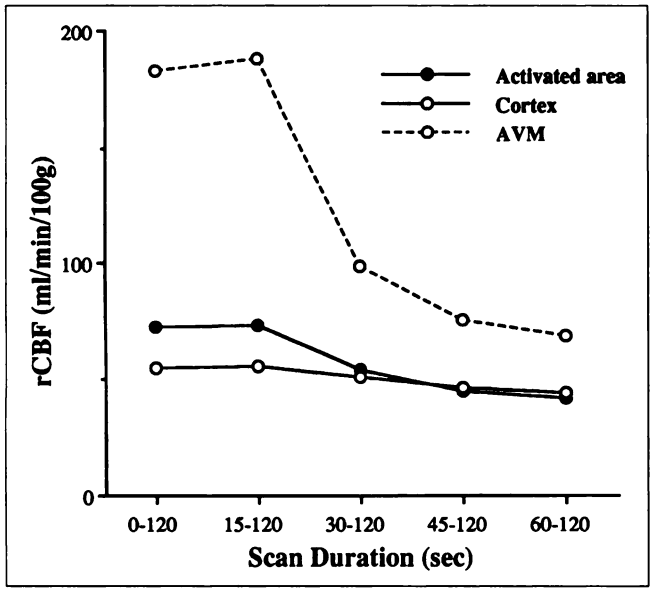

FIGURE 4. Effect of omitting the initial PET data on rCBF values in the nidus, activated area and ipsilateral gray matter (cortex) in the control scan of Patient 2. The rCBF value of the nidus significantly decreased when the initial 30 sec or more data were eliminated. Note almost stable rCBF values of ipsilateral gray matter despite shortening of the acquisition period. In the activated focus adjacent to the AVM, the effect of high activity was seen with longer scan times, including initial frames.

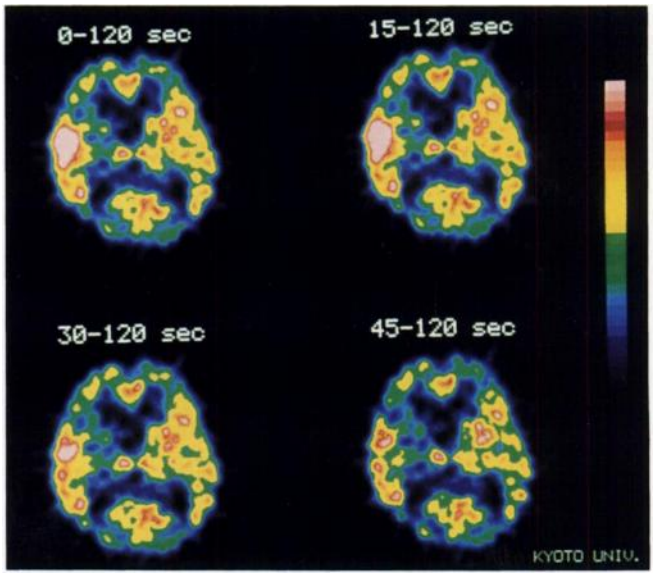

FIGURE 5. Change in the rCBF image of Patient 2 after eliminating the initial PET data. The activity of the nidus decreased gradually without affecting rCBF in other areas.

tionally important cortices. In the present study, the most adjacent location of the nidus to the activated focus was observed in Patient 2. Although the double provocation test performed during the embolization procedure was negative, transient neurological deficits occurred after surgery. The close location of the nidus and motor area seemed to be responsible for postoperative neurological deficits, since the technique for nidus extirpation was successful.

The nidus of the AVM, however, revealed high radioactivity in the ^{15}O-water study, which may interfere with activity in the activated foci adjacent to the nidus. The time-activity curves of the brain tissue demonstrate that activity in the nidus was highest between 15–45 sec (second or third frame), and the activity ratio in the nidus to the contralateral gray matter was significantly increased in the second frame. Although the rCBF image depicted the nidus as a high activity area, it did not necessarily represent increased blood flow in the AVM. Since elimination of the initial PET data provided lower estimated flow values in the nidus compared to those from complete datasets, the increased activity and earlier peak in the nidus are considered to be due to the enlarged vascular component of the AVM and its increased blood volume.

The activity ratio of the nidus to the contralateral gray matter shows that significantly high activity in the nidus affects rCBF values in the ^{15}O-water study. Figure 4 demonstrates the effect of the AVM on the nearby activated focus in rCBF. Increased rCBF in the activated area close to the AVM was considered to be caused by spillover of higher AVM activity, especially in the early period, which decreased with shorter scan times. This spillover effect was most distinct in Patient 3 who had the largest AVM.

To avoid such interference, the initial PET data should

TABLE 2
Changes in the Activated Area-to-Nearby Cortex Ratio (A/C Ratio) in rCBF and Percent Increases after Elimination of Initial PET Data

Scan duration (sec)	A/C ratio in the control scan Mean ± s.d.	A/C ratio in the activation scan Mean ± s.d.	% Increase of A/C ratio Mean ± s.d.
0–120	1.27 ± 0.41	1.40 ± 0.36	10.1 ± 13.0
15–120	1.27 ± 0.42	1.41 ± 0.36	9.7 ± 12.9
30–120	1.07 ± 0.25	1.20 ± 0.23	10.5 ± 12.0
45–120	0.96 ± 0.11*	1.09 ± 0.10*	15.0 ± 12.0
60–120	0.91 ± 0.03*	1.11 ± 0.13*	21.1 ± 12.7

*$p < 0.05$.
A/C ratio is the ratio of the activated area to the ipsilateral nearby cortex in rCBF. Significant differences were seen in scan times of 45–120 sec and 60–120 sec compared to 0–120 sec or 15–120 sec in both conditions.

TABLE 3
Changes in Increased rCBF Values and S/N Ratios in the Activated Area after Elimination of Initial PET Data*

Scan duration (sec)	Increased value of rCBF Mean ± s.d.	S/N ratio Mean ± s.d.
0–120	16.1 ± 2.2	3.81 ± 0.38
15–120	16.2 ± 2.2	3.82 ± 0.46
30–120	15.6 ± 2.9	3.50 ± 0.36
45–120	14.5 ± 2.5	2.94 ± 0.29†
60–120	11.3 ± 1.8†	1.92 ± 0.46‡

*Means and standard deviations are obtained from five activation studies.
†$p < 0.005$.
‡$p \leq 0.0001$.

be eliminated, resulting in optimal PET images. Table 2 shows improved contrast in the activated area adjacent to the nidus when the initial data are eliminated. In a study of three normal volunteers, Koeppe et al. found that the blood-borne activity component could be reduced by omitting ~40 sec of data immediately following tracer administration (*3*). Their findings demonstrated overestimation of rCBF in the large blood volume fraction, which is consistent with our results. On the other hand, for better contrast between activated foci and nonactivated areas in PET activation studies, the uptake phase of the initial 30–35 sec of data is considered to be the most important phase (*4*). The ΔCBF and S/N ratio in the activated area decreased significantly when the initial 45–60 sec of data were eliminated (Table 3). In activation studies with patients who have large vascular components, the effect of blood-borne activity on the estimated flow values should not only be avoided but also should not increase flow in the activated area. We believe that eliminating the initial 30–45 sec data avoids interference of the nidus with the activated area and provides optimal PET images.

CONCLUSION

In this study, we used the constant speed injection method of ^{15}O-water over 15 sec for 1110 MBq (30 mCi) (*10*). If we had used the bolus injection method instead, the peak time of blood activity would have been more rapid and the elimination of data from an even shorter acquisition time would provide optimal images. The greater the proximity of the lesion to the functionally important cortices, the more we need an optimal image to minimize the effect of high activity from the nidus. Delayed data acquisition can provide clearer detection of the activated area in patients with AVM, which is a useful factor in deciding the optimum treatment.

ACKNOWLEDGMENTS

The authors gratefully thank Marco Pagani, MD for editorial assistance. We also thank Masatsune Ishikawa, MD and Kazuo Yamamoto, MD for their valuable clinical assistance and suggestions.

REFERENCES

1. Leblanc R, Meyer E. Functional PET scanning in the assessment of cerebral arteriovenous malformations. *J Neurosurg* 1990;73:615–619.
2. Leblanc R, Meyer E, Bub D, Zatorre RJ, Evans AC. Language localization with activation positron emission tomography scanning. *Neurosurg* 1992;31: 369–373.
3. Koeppe RA, Hutchins GD, Rothley JM, Hichwa RD. Examination of assumptions for local cerebral blood flow studies in PET. *J Nucl Med* 1987;28: 1695–1703.
4. Volkow ND, Mullani N, Gould LK, Adler SS, Gatley SJ. Sensitivity of measurements of regional brain activation with oxygen-15-water and PET to time of stimulation and period of image reconstruction. *J Nucl Med* 1991; 32:58–61.
5. Kanno I, Iida H, Miura S, Murakami M. Optimal scan time of oxygen-15-labeled water injection method for measurement of cerebral blood flow. *J Nucl Med* 1991;32:1931–1934.
6. Hurtig RR, Hichwa RD, O'Leary DS, et al. Effects of timing and duration of cognitive activation in [^{15}O]water PET studies. *J Cereb Blood Flow Metab* 1994;14:423–430.
7. Mukai T, Senda M, Yonekura Y, et al. System, design and performance of a newly developed high-resolution PET scanner using double-wobbling mode [Abstract]. *J Nucl Med* 1988;29(suppl):877.
8. Endo M, Hukuda H, Suhara T, et al. Design and performance of PCT-3600w (15-slice type): a whole-body positron emission tomograph [Abstract]. *J Nucl Med* 1991;32(suppl):1061.
9. Kearfott KJ, Junck L, Rottenberg DA. A new headholder for PET, CT and NMR imaging. *J Comput Assist Tomogr* 1983;8:1217–1220.
10. Sadato N, Yonekura Y, Senda M, et al. Noninvasive measurement of regional cerebral blood flow change with $H_2{}^{15}O$ and positron emission tomography using a mechanical injector and a standard arterial input function. *IEEE Trans Med Imag* 1993;MI-12:703–710.
11. Herscovitch P, Markham J, Raichle ME. Brain blood flow measured with intravenous $H_2{}^{15}O$. I. Theory and error analysis. *J Nucl Med* 1983;24:782–789.
12. Raichle ME, Martin WRW, Herscovitch P, Mintun MA, Markham J. Brain blood flow measured with intravenous $H_2{}^{15}O$. II. Implementation and validation. *J Nucl Med* 1983;24:790–798.
13. Shibasaki H, Sadato N, Lyshkow H, et al. Both primary motor cortex and supplementary motor area play an important role in complex finger movement. *Brain* 1993;116:1387–1398.
14. Fox PT, Raichle ME. Stimulus rate dependence of regional cerebral blood flow in human striate cortex demonstrated by positron emission tomography. *J Neurophysiol* 1984;51:1109–1121.
15. Fox PT, Mintun MA. Noninvasive functional brain mapping by change-distribution analysis of averaged PET images of $H_2{}^{15}O$ tissue activity. *J Nucl Med* 1989;30:141–149.